INSTITUT D'AERONOMIE SPATIALE DE BELGIQUE

3 - Avenue Circulaire
B - 1180 BRUXELLES

AERONOMICA ACTA

A - N°92 - 1971

Kinetic models of the solar wind

by J. LEMAIRE and M. SCHERER

BELGISCH INSTITUUT VOOR RUIMTE-AERONOMIE

3 - Ringlaan
B - 1180 BRUSSEL

FOREWORD

This paper will be published in The Journal of Geophysical Research, Vol. 76.

AVANT-PROPOS

Ce travail sera publié dans The Journal of Geophysical Research, Vol. 76.

VOORWOORD

Deze tekst zal verschijnen in The Journal of Geophysical Research, Vol. 76.

VORWORT

Dieser Text wird in The Journal of Geophysical Research herausgegeben werden.

KINETIC MODELS OF THE SOLAR WIND

by

J. LEMAIRE and M. SCHERER

Abstract

A new kinetic model of the quiet solar wind is presented and compared with earlier exospheric, semikinetic, and hydrodynamical models. To have equal mean free paths for the protons and electrons at the baropause, the ratio of the proton temperature to the electron temperature is supposed to be $T_p(h_o)/T_e(h_o) = 0.645$. With the assumption that the trapped electrons are in thermal equilibrium with those emerging from the barosphere, the electric field distribution is calculated to cancel the electric current and space charge in the exospheric plasma. The bulk velocity, the density, the average electron and proton temperatures, and the energy flux, which are observed at 1 AU for quiet solar wind conditions, are well represented by such a kinetic model. The average electron temperature is nearly independent of the bulk velocity, whereas a positive correlation between the average proton temperature and the bulk velocity is found. Consequently it is suggested that in the interplanetary medium ($r > 6R_s$) no external heating mechanism is needed to explain the observed quiet solar wind properties. Finally, the electric field calculations in this kinetic model are found to be in reasonable agreement with the empirical electric field values deduced from observed coronal-density distribution.

Résumé

Un nouveau type de modèle cinétique du vent solaire calme est décrit et comparé aux modèles exosphériques, semi-cinétiques et hydrodynamiques antérieurs. La vitesse moyenne d'expansion, la densité, la température des électrons et des protons, ainsi que les flux d'énergie calculés correspondent de façon satisfaisante aux valeurs moyennes observées à 1 UA en période de Vent Solaire calme. On trouve également que la température des électrons est pratiquement indépendante de la vitesse du vent solaire à 1 UA tandis que la température des protons à 1 UA est corrélée positivement avec cette vitesse. Par conséquent il apparaît qu'il n'est pas nécessaire de faire appel à un chauffage extérieur du milieu interplanétaire au-delà d'une distance radiale de 6 R_s pour reproduire les conditions du Vent Solaire calme, excepté cependant pour l'anisotropie des températures qui peut être réduit par des instabilités de plasma (firehose). La distribution du champ électrique calculée pour maintenir dans ces modèles cinétiques la quasi-neutralité et l'égalité des flux d'échappement des électrons et des ions est en accord satisfaisant avec celle déduite des densités électroniques observées dans la couronne solaire.

Samenvatting

Een kinetisch model is ontwikkeld voor de zonnewind tijdens een kalme periode van zonneactiviteit. De bekomen resultaten worden vergeleken met de reeds bestaande exosferische, semi-kinetische en hydrodynamische modellen. De snelheid, de deeltjes dichtheid, de gemiddelde elektron en proton temperatuur, en de energieflux, waargenomen op 1 A.E., worden goed benaderd in zulk kinetisch model. De gemiddelde elektron temperatuur is praktisch onafhankelijk van de zonnewind snelheid. Tussen de proton temperatuur en deze snelheid bestaat echter een positieve correlatie. Dit wijst op een mogelijke verklaring van de zonnewind eigenschappen in de interplanetaire ruimte ($r > 6R_s$), waarbij geen uitwendig verwarmingsmechanisme vereist is. Tenslotte levert de berekening van het elektrische veld in dit kinetisch model, resultaten welke behoorlijk overeenstemmen met de proefondervindelijke waarden, welke afgeleid worden van waargenomen elektron dichtheidsdistributies.

Zusammenfassung

Ein neues kinetisches Model des Sonnenwindes ist beschrieben und mit vorherigen exosphärischen, semi-kinetischen und hydrodynamischen Modelen verglichen. Die Geschwindigkeit, Dichte, Electron-und Proton - Temperaturen sowie die Energie Ausflüsse sind in Uberstimmung mit den Beobachtungen des stillen Sonnenwindes. Die Berechneten Electronen - Temperaturen sind ungefähr unabhängig von der Geschwindigkeit in der Nähe 1 AE. Die berechneten Protonen - Temperaturen haben eine positive Wechselbeziehung mit der Sonnenwind Geschwindigkeit. Die Beobachtungen haben die selben Eigenschaften gezeigt. Deshalb is es weiter nicht nötig ein Heizungmechanismus des Sonnenwindes zu suchen für $r > 6R_s$, um die meisten Eigenschaften des Sonnenwindes zu finden. Das electrische Feld in solch eines kinetisches Model ist in genügender Uberstimmung mit was von der beobachteten Electronen-Dichte erfolgt.

1. INTRODUCTION

To obtain a kinetic description of the solar wind phenomena, several authors have applied exospheric theories to the collisionless region of the solar corona. Chamberlain [1960] assumed above a given altitude (called critical level, exobase, or baropause) the coronal particles move freely under the influence of an electric potential field $\Phi_E(r)$ and the solar gravitational field $\Phi_g(r) = -GM/r$; r is the radial heliocentric distance; $M = 1.989\ 10^{33}$ grams and $G = 6.668\ 10^{-8}$ dyne $cm^2\ g^{-2}$.

To ensure the electrical charge neutrality in the coronal exosphere, i.e.,

$$n_p(r) = n_e(r) \tag{1}$$

where n_p and n_e are the proton and electron number density, respectively, Chamberlain assumed that $\Phi_E(r)$ is given by the Pannekoek-Rosseland's formula [Pannekoek, 1922; Rosseland, 1924]

$$\Phi_E(r) - \Phi_E(r_o) = -\frac{m_p - m_e}{2e}\left[\Phi_g(r) - \Phi_g(r_o)\right] \tag{2}$$

corresponding to a collision-dominated plasma in hydrostatic equilibrium [Van de Hulst, 1953]. In (2), m_p and m_e denote the proton and electron mass, respectively, and e is the electronic charge. The same electric potential is also used by Jensen [1963], Brandt and Cassinelli [1966], Dessler [1969], Eviatar and Schulz [1970], and Brandt [1970]. For such an electrostatic potential distribution, however, the escape flux of the electrons F_e would be 43 times larger than the escape of the protons F_p

Sen [1969] constructed a simplified model exosphere of the corona in which a finite electric sheath potential was assumed at the baropause (called the exospheric surface by Sen) to maintain the equality of the escaping fluxes of the protons F_p and of the electrons F_e

$$F_p(r_o) = F_e(r_o) \qquad (3)$$

In this model the electric field is about twice as large as the Pannekoek-Rosseland's field. Although Sen [1969] does not explicitly give the electrostatic potential distribution, his results can be found by assuming that, for $r > r_o$,

$$\Phi_E(r) - \Phi_E(r_o) = -\psi_o \left(2 - \frac{r_o}{r}\right)$$

$$= \beta_s \frac{m_p \Phi_g(r_o)}{e} \left(2 - \frac{r_o}{r}\right) \qquad (4)$$

where ψ_o and β_s are constants determined by solving (3). With a constant value of β_s or ψ_o, however, the quasi-neutrality condition (1) cannot be satisfied in the exosphere. Recently, Lemaire and Scherer[1969] presented exospheric models for the terrestrial polar ion exosphere in which the quasi-neutrality and zero-electric-current conditions (1) and (3) are both satisfied simultaneously. The electric potential in their kinetic theory is given by

$$\Phi_E(r) - \Phi_E(r_o)$$

$$= \left[\alpha - \beta(r) \frac{r_o}{r}\right] \frac{m_p \Phi_g(r_o)}{r} ; \quad (r > r_o) \qquad (5)$$

where α is a constant and $\beta(r)$ is a monotonic function of the radial distance. Formula (4) can be obtained from equation (5) by assuming that $\beta(r) = \beta_s$ = constant and $\alpha = 2\beta_s$; Pannekoek's [1922] potential distribution (2) is recovered from (5) when $\alpha = \beta(r) = 1/2\ (m_p - m_e)/m_p$.

As shown by Lemaire and Scherer[1970], the escape flux of the electrons at the critical level is determined by the height of the total potential barrier.

$$m_e [\Phi_g(\infty) - \Phi_g(r_o)] - e[\Phi_E(\infty) - \Phi_E(r_o)]$$

$$\simeq -\alpha m_p \Phi_g(r_o)$$

the escaping electrons have to overcome. Therefore, the escape flux of the electrons (and protons) depends only on the value of α and not on $\beta(r)$. The particle density distributions are functions of both parameters $\beta(r)$ and α. Hence the constant α can be determined so that the condition (3) is satisfied. The quasi-neutrality condition (1) then yields a transcendental equation in $\beta(r)$, which can be solved numerically at each level r and determines the shape of the electric potential distribution in the whole exosphere.

The radial distribution of the electric potential given in volts, for a coronal temperature $T(r_o) = 10^6$ °K at the critical level $r_o = 6.05$ R_s is plotted in Figure 1 (LSa). Chamberlain's [1960] (PR) and Sen's [1969] (S) counterparts are also shown. A radial magnetic field configuration is assumed in all models discussed in this paper.

Recently, Jockers [1970] and Hollweg [1970] proposed a 'semikinetic' theory for the exospheric region of the solar wind. They considered a collisionless or kinetic description for the protons and an hydrodynamical treatment for the electron gas. Indeed, they determined $\Phi_E(r)$, the electric potentials in the exosphere, by integrating and solving the equation

$$e \frac{d\Phi_E(r)}{dr} = -\frac{1}{n_e} \frac{d(n_e k T_e)}{dr} \qquad (8)$$

which is a simplified form of the hydrodynamical equation of motion for the electrons. They also assumed the electron temperature T_e to be a known function of r. For instance, in Jocker's Model III the electron temperature is given by $T_e(r) = 1.32\ 10^6$ °K for $r < 9\ R_s$, and by $T_e \alpha\ r^{-1/3}$ for $r > 9\ R_s$, The proton baropause level is supposed to be at $r_o = 2.5\ R_s$, and the velocity

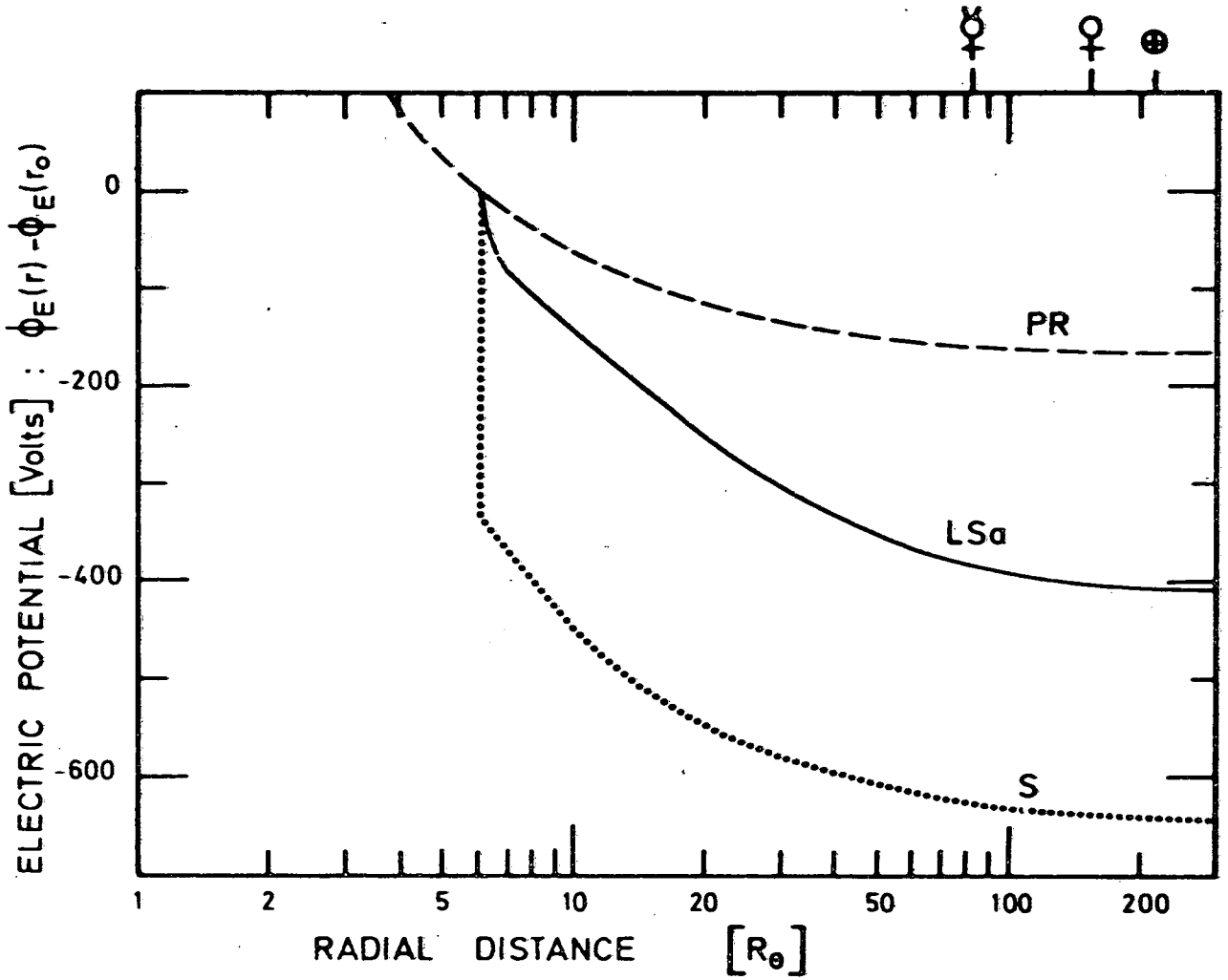

Fig. 1.- The electric potential in some exospheric models of the solar corona. The dashed line (PR) illustrates the Pannekcek-Rosseland's distribution ; the dotted curve (S) gives Sen's exospheric model for a baropause $r_o = 6.05\ R_\odot$ and a temperature $T(r_o) = 10^6\,°K$; the solid line (LSa) corresponds with the kinetic models of Lemaire and Scherer for the same baropause conditions.

distribution at this boundary is Maxwellian and symmetric.

In Hollweg's [1970] models the electron gas is supposed to be isothermal [$T_e(r) = c^{te}$] and the proton distribution at the baropause ($r_o = 10 - 20\ R_s$) is Maxwellian but asymmetric, i.e., the protons are assumed to move with an initial bulk velocity U. The value of U was chosen to be equal to the expansion velocity of Hartle and Sturrock's [1968] two-fluid model.

In these semikinetic models, the electron baropause is located at infinity and the escaping electrons have to overcome a potential barrier : $- e [\Phi_E(\infty) - \Phi_E(r_o)] = \infty$ when $T_e(r)$ is a constant.

1. DETERMINATION OF BOUNDARY CONDITIONS.

To calculate the electric potential energy for each kind of particles with mass m_j and charge $Z_j e$, the explicit expressions for the escape fluxes and densities in the exosphere must be known.

Approximating the actual velocity distribution at the baropause r_o by a symmetric Maxwellian one, Lemaire and Scherer [1971] have determined the velocity distribution at any exospheric level r by means of Liouville's theorem. More general distribution functions at the baropause have also been considered by the authors, for instance, the asymmetric Maxwellian velocity distribution function.

$$F_j(\vec{v}, r_o;\ N_j,\ \theta_j,\ \vec{U}_j) = N_j \left(\frac{m_j}{2\pi k \theta_j} \right)^{3/2} . \exp \left[- \frac{m_j (\vec{v} - \vec{U}_j)^2}{2k\theta_j} \right] \qquad (9)$$

where N_j, θ_j, and $\vec{U}_j$ are parameters determined by appropriate boundary conditions [Lemaire and Scherer, 1971].

Calculating the moments of the distribution function, one obtains explicit expressions for the particle density $n_j(r)$, the flux $F_j(r)$, the pressure tensor components $p_{\parallel j}(r)$ and $p_{\perp j}(r)$, ... With these quantities, we calculate the bulk velocity $w_j(r) = F_j(r)/n_j(r)$, the longitudinal and transverse temperatures $T_{\parallel j}(r) = p_{\parallel j}(r)/ kn_j(r)$ and $T_{\perp j}(r) = p_{\perp j}(r)/kn_j(r)$, and the average temperature $\langle T_j(r)\rangle = (1/3)[T_{\parallel j}(r) + 2T_{\perp j}(r)]$ [Lemaire and Scherer, 1971].

To compute a solar wind model with these formulas, we must first choose the baropause altitude h_o. The baropause is generally defined as the surface where the mean free path l becomes equal to the density scale height H

$$l(h_o) = H(h_o) \tag{10}$$

From photometric and polarimetric observations of the solar corona during an eclipse, it is possible to deduce the electron density distribution for $h < 20\ R_s$. An example of such a radial density profile is given by Pottasch [1960] for a period of minimum in the sunspot cycle. From this density distribution shown by curve 1 in Figure 2, it is possible to calculate the scale height

$$H(h) = \left(-\frac{d \ln n_e}{dh} \right)^{-1} \tag{11}$$

The result is given by curve 2 in Figure 2.

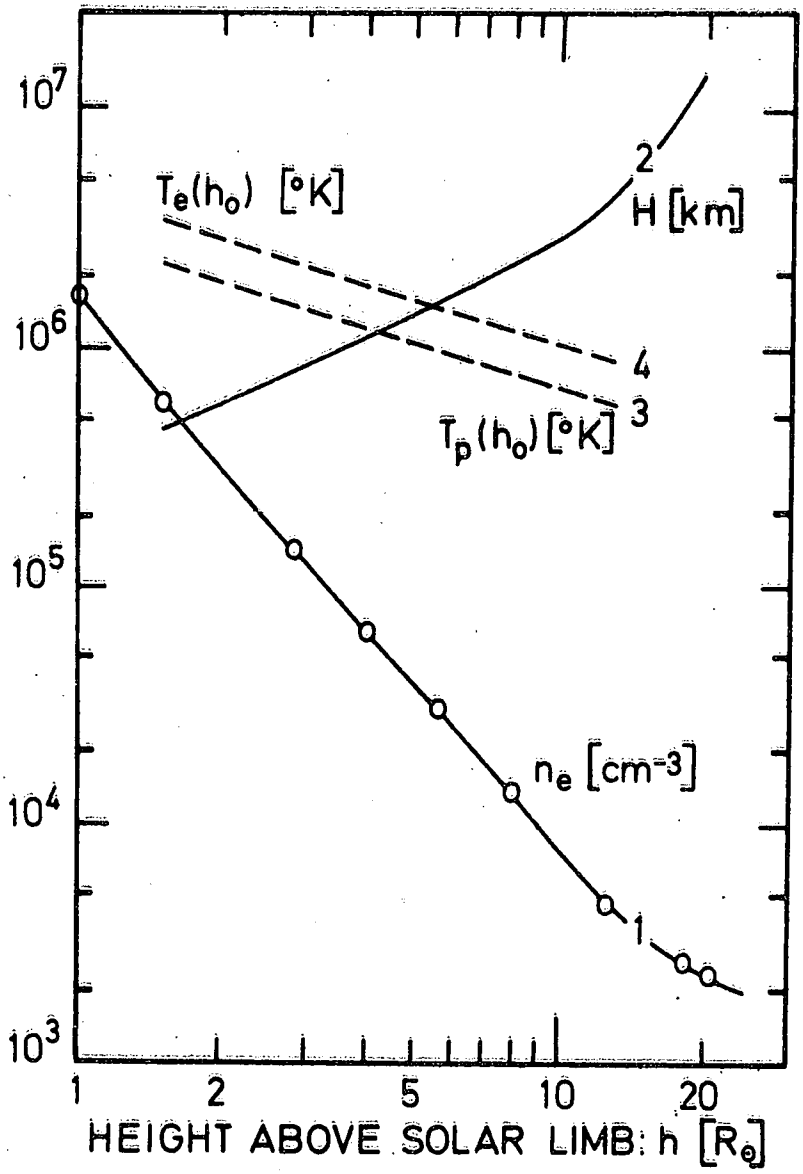

Fig. 2.- Curve 1 shows the equatorial electron density distribution (cm^{-3}) in the solar corona observed during an Eclipse near the minimum in the sunspot cycle as reported by Pottasch [1960] ; curve 2 gives the corresponding density scale height H in km ; curves 3 and 4 respectively illustrate the proton and electron temperatures at the baropause as a function of the baropause altitude h_o expressed in solar radii.

On the other hand, following Spitzer [1956] and Nicolet et al. [1971], who generalized the mean free path (m.f.p.) theory for unequal electron and proton temperatures, it can be shown that $(l_D)_p$, the deflection m.f.p. of thermal protons, is given by

$$(l_D)_p = 1.8 \times 10^5 \frac{T_p^2}{n_e \ln \Lambda_{pp}} \text{ cm} \qquad (12)$$

where the Coulomb logarithm, $\ln \Lambda_{ij}$, for $(i - j)$ collisions is defined by Nicolet et al. [1971] as

$$\ln \Lambda_{ij} = \ln \left[\frac{k^3 T_i^3}{\pi n_e (1 + T_i/T_j) e^6} \right]^{1/2} \qquad (13)$$

For the temperatures and densities considered in the various models, $\ln \Lambda_{ij}$ is practically constant and equal to 25.

Hence, for a given value of the temperature T_p, the altitude h_o of the proton baropause can be determined by solving (10), where $l(h_o)$ is replaced by $(l_D)_p$ defined in (12).

Inversely, the expressions (10) and (12) can be used to determine the required proton temperature at an altitude h_o, and thus the thermal protons are collisionless for $h > h_o$. This baropause temperature $T_p(h_o)$, is given by

$$\log T_p(h_o) = \frac{1}{2} \log n_e(h_o) + \frac{1}{2} \log H(h_o) + 0.57 \qquad (14)$$

where n_e and H are given respectively in cm^{-3} and km.

Curve 3 in Figure 2 shows the result obtained when $n_e(r)$ and H(r) are taken from Pottasch's [1960] observed density distribution. From this curve, it can also be seen that, if $T_p(h_o) \leq 6 \times 10^5$ °K, the collision-dominated region for the protons extends to radial distances greater than

20 R_s for coronal conditions corresponding to a minimum of solar activity [Pottasch, 1960].

To determine the electron baropause we use the deflection m.f.p. of a thermal electron in an hydrogen plasma, which is defined by

$$(l_D)_e = 0.416(T_e/T_p)^2(l_D)_p \qquad (15)$$

When the electron and proton temperatures are equal, the electron m.f.p. is smaller than the proton m.f.p. and the collision-dominated region for the electrons extends to a higher altitude ($h_{o,e}$) than the region for the protons ($h_{o,p}$) extends.

It is convenient, and not unreasonable, to assume that the escaping electrons and protons come from the same coronal layer, and therefore their respective baropause altitudes are the same. This implies

$$[l_D(h_o)]_e = [l_D(h_o)]_p \qquad (16)$$

or, considering (12) and (15),

$$T_p(h_o)/T_e(h_o) = 0.645 \qquad (17)$$

Since the mean collision frequency for angular deflections of protons $(\nu_D)_p$ is much larger than the mean collision frequency for energy equipartition between protons and electrons ν_{eq} [Spitzer, 1956], it is reasonable to assume unequal temperatures for the electrons and protons at the baropause level [Hartle and Sturrock, 1968].

From relation 17 and curve 3 in Figure 2, it follows that the electron temperature at the baropause is also related to the altitude of the baropause. This relation is illustrated by curve 4 in Figure 2, which can be used to determine the baropause altitude h_o for a given value of $T_e(h_o)$.

For $T_e(h_o) = 1.4 \times 10^6$ °K, then $h_o = 6.3\ R_s$; from curve 1, $n_e(h_o) = 2.3 \times 10^4\ cm^{-3}$, and from curve 3, $T_p(h_o) = 0.9 \times 10^6$ °K.

Since the potential energy of the electrons is an increasing function of altitude, they can be classified in four conventional classes according to the characteristics of their orbits: (a) The escaping electrons that have enough kinetic energy to overcome the potential barrier; (b) the ballistic electrons that emerge from the barosphere but cannot escape; (c) the trapped electrons that have two mirror or reflection points in the exosphere; and finally (d) the incoming electrons. In what follows, we neglect the incoming particles and assume that the trapped electrons are in thermal equilibrium with those emerging from the barosphere. This assumption implies the existence of some slow scattering mechanisms (particle-particle interaction, recombination, . . .) that feed and depopulate the trapped orbits continuously.

For the protons, however, the potential energy is a decreasing function of altitude. As a consequence, there are no trapped or ballistic protons, and in the kinetic models considered in this paper, all the protons are escaping.

For an asymmetric velocity distribution, the electron and proton temperatures and densities at the baropause are related to the parameters θ_j, N_j, and U_j by

$$\lim_{r \to r_o^+} T_{\perp e}(r) = a\theta_e \qquad \lim_{r \to r_o^+} T_{\perp p}(r) = \theta_p$$

$$\lim_{r \to r_o^+} n_e(r) = bN_e \qquad \lim_{r \to r_o^+} n_p(r) = cN_p \qquad (18)$$

where a, b, and c are given in Appendix A as functions of θ_j, N_j, and U_j. These constants result from the truncation of the proton and electron velocity distribution such that the incoming particles are excluded.

The left-hand sides of these equations are the actual temperatures $T_{\perp e}(r_o)$, $T_{\perp p}(r_o)$ and densities $n_e(r_o)$, $n_p(r_o)$ at the heliocentric distance r_o. Therefore, we obtain from (18) simple relations between the parameters θ_j, N_j, and the boundary conditions $T_j(r_o)$, $n_j(r_o)$. For practically all of our models, the numerical value of a is equal to 0.97, and thus (17) and (18) yield

$$\theta_e = T_{\perp e}(r_o)/0.97, \quad \theta_p = T_{\perp e}(r_o)\ 0.645$$
$$N_e = n_e(r_o)/b\ , \quad N_p = n_e(r_o)/c \tag{19}$$

Moreover, since the solar-wind velocity is always much smaller than the electron thermal speed, the velocity distribution of the electrons is nearly isotropic, and U_e can be taken equal to zero. For the protons, however, the mean flow velocity at the baropause is nearly sonic and the distribution function can be highly asymmetric. Therefore, the parameter U_p is not negligible.

3. KINETIC MODEL OF SOLAR WIND.

Our interpretation of the parameters N_j, θ_j, U_j, characterizing the velocity distribution 9, is quite different from the signification Jockers [1970] and Hollweg [1970] give to thesequantities. These authors identify N_j, θ_j, and U_j, respectively, with the densities $n_j(r_o)$, the temperatures $T_j(r_o)$, and the wind velocity $w_j(r_o)$ just below the baropause boundary.

In our kinetic approach, the velocity distribution given by (9), or even a more general function, is essentially a convenient boundary value for Liouville's equation. The parameters N_j, θ_j, and U_j can be determined to fit the densities $n_j(r_o^+)$, the temperatures $T_j(r_o^+)$, and the bulk velocity $w_j(r_o^+)$ just above the baropause, to the 'observed' values at $r = r_o$. Hence, in our models no zero-order discontinuity exists at the baropause for the lower-order moments of the velocity distribution.

In Figures 3 and 4 we give the bulk velocity and the electron density at 1 AU versus the electron temperature at the baropause $T_e(r_o)$ and the value of the parameter U_p, respectively. The calculated flow speed at 1 AU increases rapidly with $T_e(r_o)$ but does not change significantly with U_p. Therefore, a rather precise value of $T_e(r_o)$ can be determined by fitting W_E, the bulk velocity at 1 AU, to the observed solar-wind flow speed.

The average proton and electron temperatures at 1 AU versus the electron temperature at the baropause $T_e(r_o)$ and the value U_p are illustrated in Figures 5 and 6, respectively. The calculated electron temperature $\langle T_e \rangle$ does not change very much with $T_e(r_o)$ or with U_p. The proton temperature, however, depends strongly on both of these parameters. Hence, taking into account the results of Figure 3 and 5, we conclude that there exists a positive correlation between the flow speed W_E and $\langle T_p \rangle_E$, where, on the contrary, the electron temperature $\langle T_e \rangle_E$ is nearly independent of W_E. These important properties of our kinetic models are well supported by the conclusions obtained from solar-wind observations by Montgomery et al. [1968], Burlaga and Ogilvie [1970], and Hundhausen et al. [1970].

As will be discussed in a forthcoming paper, the relation of $T_{p,E}$ and W_E departs slightly from the observed one for the small and large solar-wind velocities we considered, i.e., when $T_e(r_o)$ is lower than 1.2×10^6 °K and higher than 2×10^6 °K. The reason for this is that

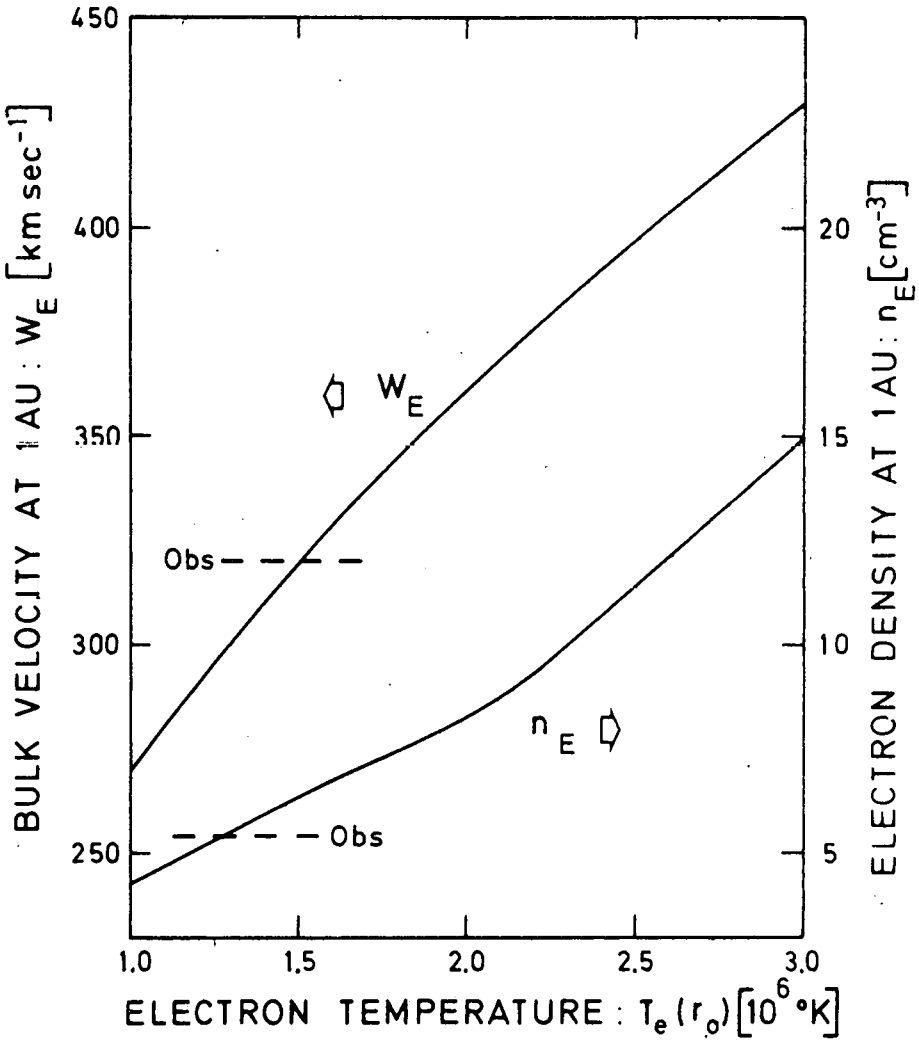

Fig. 3.- The bulk velocity W_E (left hand scale), and the electron density n_E (right hand scale) at 1AU for $U_p = U_e = 0$ versus the electron temperature at the baropause. The observed (Obs) quiet solar wind flow speed and density are also plotted.

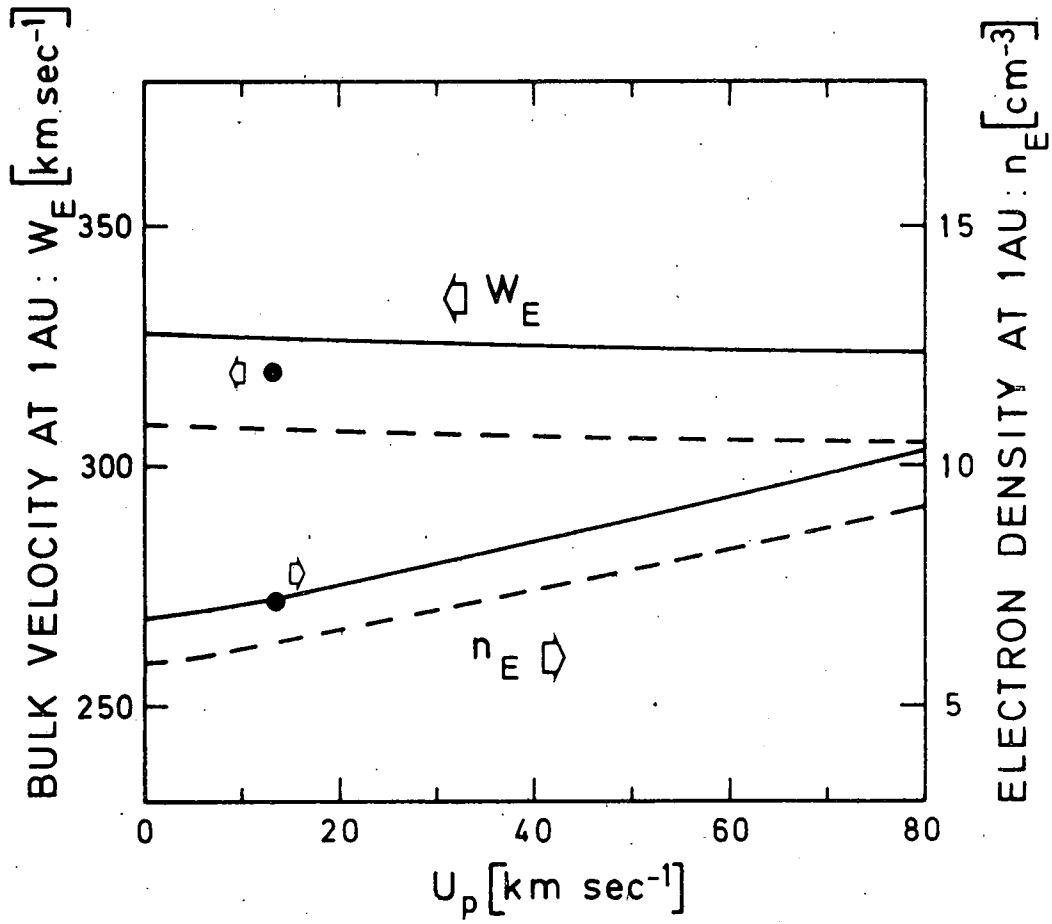

Fig. 4.- The bulk velocity W_e (left hand scale), and the electron density n_E (right hand scale) at 1 AU, versus U_p. The dashed and solid lines correspond to an electron temperature at the baropause of respectively 1.4×10^6 °K and 1.6×10^6 °K. The dots illustrate the model LSb which corresponds with the baropause conditions $r_o = 6.6\ R_\odot$, $T_e(r_o) = 1.52 \times 10^6$ °K, $T_p(r_o) = 0.984 \times 10^6$ °K, $U_e = 0$, $U_p = 14$ km sec^{-1}, and $n_e(r_o) = 3.1 \times 10^4$ cm^{-3}.

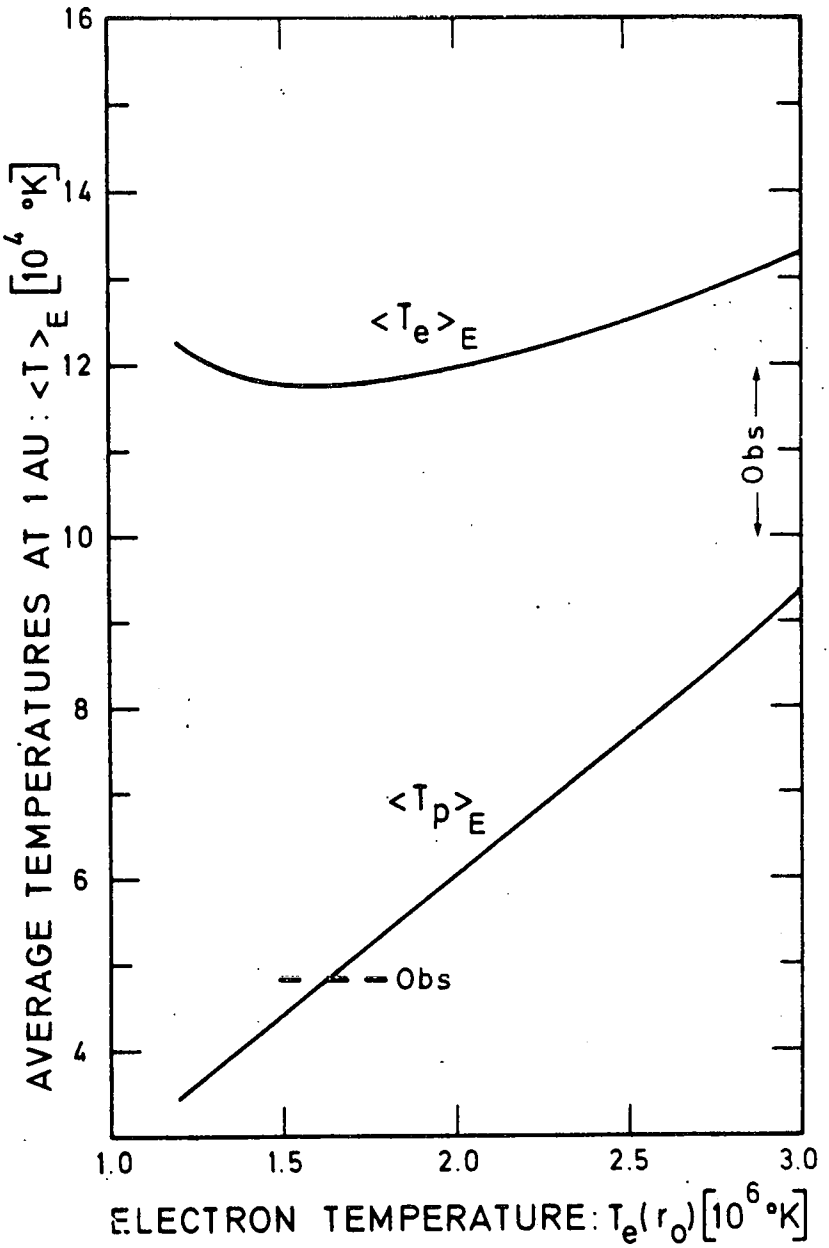

Fig. 5.- The average electron and proton temperatures at 1 AU and for $U_p = U_e = 0$, versus the electron temperature at the baropause. The observed (Obs) quiet solar wind values are also plotted.

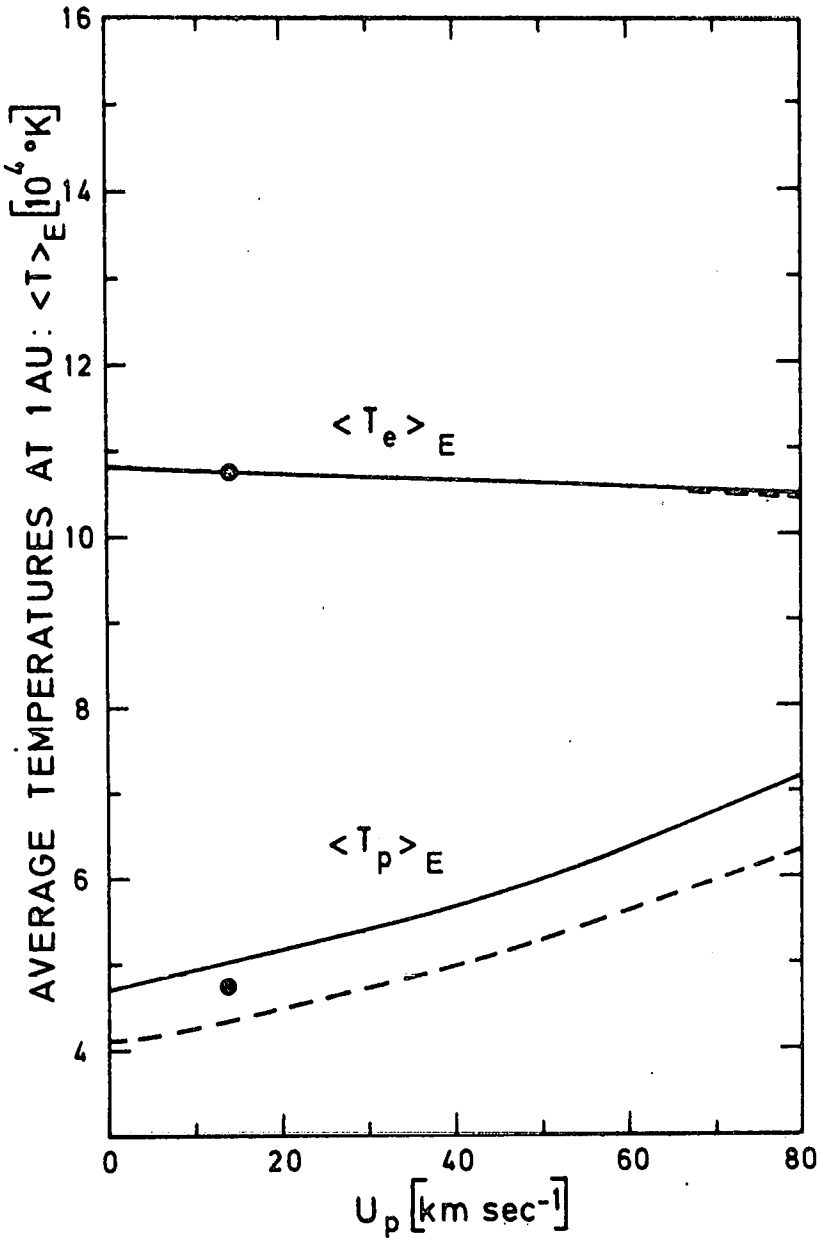

Fig. 6.- The average electron and proton temperatures at 1 AU, versus U_p. The dashed and the solid lines correspond respectively to an electron temperature at the baropause of 1.4×10^6 °K and 1.6×10^6 °K. The dots illustrate the model LSb which corresponds with the baropause conditions $r_o = 6.6\ R_\odot$, $T_e(r_o) = 1.52 \times 10^6$ °K, $T_p(r_o) = 0.984 \times 10^6$ °K, $U_e = 0$, $U_p = 14$ km sec^{-1}, and $n_e(r_o) = 3.1 \times 10^4$ cm^{-3}.

the actual density distribution in a cold or a hot streamer differs from the observed one illustrated by curve 1 in Figure 2. As a consequence, the baropause altitude corresponding to small or large values of $T_e(h_o)$ is probably different from the value deduced in the previous section by using Pottasch's observed average densities. This difference can also explain the discrepancy between the relation of n_E and W_E (Figure 3) and the actual observed relation [Hundhausen et al., 1970].

In Table 1 we summarize the observed solar-wind flow speed W_E, the particle flux F_E, the density n_E, the average temperatures $\langle T_e \rangle_E$ and $\langle T_p \rangle_E$, the temperature anisotropies $(T_{\parallel}/T_{\perp})_p$, the total kinetic energy flux E_E and the heat conduction flux C_E for quiet solar-wind conditions as they have been reported by Hundhausen [1968, 1969, 1970]. We also give the corresponding values computed in our kinetic model LSb, which, at the baropause level $r_o = 6.6\ R_s$, has the density and proton temperature of $n_e(r_o) = 3.1 \times 10^4\ cm^{-3}$ and $T_p(r_o) = 0.984 \times 10^6\ °K$, respectively. The electron temperature $T_e(r_o)$ and the value of the parameter U_p are $1.52 \times 10^6\ °K$ and 14 km sec^{-1}, respectively. They were chosen to obtain at 1 AU a flow speed and proton temperature that are the most probable values for quiet solar-wind conditions, 320 km sec^{-1} and $4.8 \times 10^4\ °K$ [Hundhausen, 1968]. For this model, the bulk velocity just above the baropause is $W(r_o^+) = 77.5$ km sec^{-1}.

It can be seen from Table 1 that the average electron temperature is equal to $11.7 \times 10^4\ °K$, which is in good agreement with the observed values. The density n_E and the particle flux F_E are also in relatively good agreement with the solar-wind observations. The density excess of 30% is small as compared with the dispersion of the various experimental determinations [Hundhausen et al., 1970]. The total kinetic energy flux which is mainly transported by the protons is also in close agreement with the observed 0.24 erg cm^{-2} sec^{-1} [Hundhausen, 1970]. Finally, Table 1 also shows that the computed thermal-conduction flux (mainly transported by the electrons) is of the same order of magnitude as the experimental

TABLE 1. Comparison of the Quiet Solar-Wind Conditions with the Results of the Kinetic Model LSb, which is a best fit solution to these quiet Solar-Wind Conditions.

Conditions	Hundhausen [1968,1969,1970]	Kinetic Model LSb	Units
W_E	320	320	km sec^{-1}
n_E	5.4	7.18	cm^{-3}
F_E	1.73	2.30	cm^{-2} sec^{-1}
$< T_e >_E$	10 to 12 x 10^4	11.7 x 10^4	°K
$< T_p >_E$	4.8 10^4	4.8 x 10^4	°K
$(T_{\parallel}/T_{\perp})_e$	1.1 to 1.2	3.05	
$(T_{\parallel}/T_{\perp})_p$	3.4	164	
E_E	2.4 x 10^{-1}	2.0 x 10^{-1}	erg $cm^{-2}sec^{-1}$
C_{eE}	1 x 10^{-2}	5.1 x 10^{-2}	erg $cm^{-2}sec^{-1}$

estimations given by Montgomery et al. [1968].

Since the experimental temperatures are often deduced from the dispersion of the energy spectra, it is convenient to define the half-width temperatures $\overline{T}_{\perp}$, $\overline{T}_{\uparrow\uparrow}$, and $\overline{T}_{\downarrow\downarrow}$ which characterize the dispersion of the velocity distribution in a direction perpendicular, parallel, and anti-parallel to the magnetic field, respectively (see Appendix B). In the model LSb, the numerical values of these half-width temperatures for the protons are given by

$$\overline{T}_{\perp} = 1.4 \times 10^4 \text{ °K}$$

$$\overline{T}_{\uparrow\uparrow} = 5.1 \times 10^4 \text{ °K}$$

$$\overline{T}_{\downarrow\downarrow} = 1.8 \times 10^4 \text{ °K}$$

which shows that the dispersion of the velocity distribution for the

protons is significantly larger in the outward direction than in the antiparallel direction ($\bar{T}_{\uparrow\uparrow} = 2.8\ \bar{T}_{\downarrow\downarrow}$). The value of the ratio of the parallel to the perpendicular half-width temperature ($\bar{T}_{\uparrow\uparrow}/\bar{T}_{\perp} = 3.6$) is relatively small and is comparable to the observed temperature anisotropy. This small value is due to the rather weak asymmetry in the proton velocity distribution at the baropause ($U_p = 14$ km).

The corresponding ratio of the 'integrated' temperatures [$(T_{\parallel}/T_{\perp})_p = 164$], which is equivalent with the ratio of the parallel to the perpendicular kinetic pressure, is, however, much larger than the observed proton value (~3.4). For the electrons this ratio is much smaller [$(T_{\parallel}/T_{\perp})_e = 3$]. This small ratio is a consequence of the large number of trapped electrons as compared with the number of escaping electrons at 1 AU. The value of the electron temperature anisotropy is also much larger than the observed ones (1.1 - 1.2). Since the computed pressure anisotropies are quite large and since the ratio β of the kinetic pressure to the magnetic pressure at 1 AU is approximately equal to 0.7 for 6-γ magnetic field intensity , plasma instabilities could become important [Kennel and Scarf, 1968; Eviatar and Schulz, 1970; Hollweg and Völk, 1970; Forslund, 1970; Bertotti et al., 1971; Pilipp and Völk, 1971]. It can be verified that the model LSb, i.e., $\beta_{\parallel p} = 0.7$, $(T_{\parallel}/T_{\perp})_p = 164$, $(T_{\parallel}/T_{\perp})_e = 3$, $T_{e\parallel}/T_{p\parallel} = 1.51$, is stable in the small wave number limit. W. Pillip (personal communication, 1971), has calculated that under these conditions the maximum growth rate occurs for right-hand polarized waves with a frequency of 0.14 sec^{-1} and a wavelength of 520 km. The characteristic growth time for these unstable waves is equal to 2×10^3 sec.

If the average temperatures can be predicted correctly by a collisionless model, the electro-magnetic waves generated in such a model would change the pitch-angle distribution of the particles but not their mean kinetic energy.

Moreover, it has been suggested by W. I. Axford (personal communication, 1971) that Coulomb collisions could contribute significantly to reduce the anisitropy of the velocity distribution in the vicinity of the earth. Indeed, the mean Coulomb deflection times of the solar-wind protons ($T_p = 4.8 \times 10^4$ °K) and the thermal electrons $T_e = 11.7 \times 10^4$ °K) are respectively, $(t_D)_p = 6.6 \times 10^5$ sec and $(t_D)_e = 4 \times 10^4$ sec [Spitzer, 1956]. These values are larger than but still comparable to the time required by a proton and a thermal electron, respectively, to travel a distance equal to the density scale height ($H \simeq 0.5$ AU) : $(t_H)_p = 2.5 \times 10^5$ sec and $(t_H)_e = 3.4 \times 10^4$ sec. Therefore, the Coulomb collisions may contribute significantly to the pitch-angle scattering of the particles, especially for the lower-energy electrons. This contribution can substantially reduce the temperature anisotropies obtained in collisionless models. The collision time (t_{eq}) for energy equipartition between electrons and protons is about 43 times larger than $(t_D)_p$ and 100 times larger than $(t_H)_p$: $t_{eq} \simeq 3 \times 10^7$ sec [Spitzer,1956]. As a consequence, at 1 AU no significant energy can be transfered from the electrons to the protons by Coulomb collisions. Therefore, Coulomb collisions could provide the wanted mechanism to reduce the temperature anisotropy without changing the average temperature or mean kinetic energy of the protons and electrons at 1 AU.

4. COMPARISON WITH EARLIER MODELS

Table 2 gives the flow velocity, density flux, average temperature, and pressure or temperature anisotropy for different exospheric and hydrodynamical models. It can be seen that the exospheric models are not as bad as it was thought during the last decade. Indeed, a self-consistent calculation of the electric field and an appropriate determination of the boundary conditions gives a satisfactory description of the quiet solar wind at 1 AU. Although we neglected wave-particle interactions and Coulomb collisions, our kinetic solar wind model predicts (a) the correct

average electron and proton temperatures; (b) a larger half-width temperature in the outward direction than in the antiparallel one; (c) an electron temperature nearly independent of the flow speed; (d) a positive correlation between the average proton temperature and the flow velocity at 1 AU; (e) a rather representative value for the total kinetic-energy flux and heat conduction at 1 AU.

5. ELECTRIC FIELD IN THE SOLAR CORONA

We showed that the electric potential $\Phi_E(r)$ can be determined by using the zero-electric-current and quasi-neutrality conditions 3 and 1. The electric field follows from $\vec{E} = \vec{\nabla}\,\Phi_E(r)$.

This field is directed outward and has an intensity larger than the usually used Pannekoek's value.

$$E = \frac{1}{2}\, m_p g/e$$

where g denotes the gravitational acceleration [Lemaire and Scherer, 1969]. The extremely small charge separation necessary to support this electric field can be obtained from Poisson's equation

$$\vec{\nabla}^2 \Phi_E = -4\pi e(n_p - n_e) \qquad (20)$$

Since the protons are more heavily attracted by the sun's gravitational field than the electrons are ($m_p \gg m_e$), the gravitational force establishes a minute positive space charge, which in the collision-dominated region of the corona is given by

$$\frac{n_p - n_e}{n_e} = \frac{G m_p^2}{2e^2} \approx 4 \times 10^{-37} \qquad (21)$$

In the exospheric region, however, the space charge becomes negative and much more pronounced (of the order of 10^{-21}). The reason is that the more speedy electrons tend to escape at the baropause and try to fill the outer space more rapidly than the heavy ions,

$$\langle c_p \rangle = (8kT_p/\pi m_p)^{1/2} \ll (8kT_e/\pi m_e)^{1/2} = \langle c_e \rangle$$

In Figure 7 we plotted the ratio of the electric to the gravitational force acting on a proton. The values of $eE/m_p g$ can also be determined for $r < 20R_s$ from Pottasch's [1960] observed electron-density distribution (see Figure 2). In a pure H^+ isothermal corona the electric field is also given by

$$eE = -\, kT_e \vec{\nabla} \ln n_e \qquad \text{with } (T_{\parallel}/T_{\perp})_e = 1 \tag{22}$$

which is equivalent with (8) used by Jockers [1970], and Hollweg [1970]. From the scale height definition (11), it follows that

$$eE/m_p g = (kT_e/m_p g)[1/H(r)] \tag{23}$$

where H(r) is given in Figure 2 for a minimum in the sunspot cycle. The empirical results for $T_e = 1.52 \times 10^6$ °K are also shown in Figure 7. The agreement between the theoretical and experimental points is quite satisfactory if we consider that we have neglected temperature gradients and the presence of heavier ions.

TABLE 2. Data of Various Kinetic, Semikinetic , and Hydrodynamical Solar Wind Models

Models	W_E, km sec^{-1}	n_E, cm^{-3}	F_E, cm^{-2} sec^{-1}	$\langle T_e \rangle_E$ °K	$\langle T_p \rangle_E$ °K	$T_{\parallel e}/T_{\perp e}$	$T_{\parallel p}/T_{\perp p}$
Ch[1]	20	370	7.4×10^8	11×10^4	11×10^4		
S[2]	258	3.34	0.86×10^8				
LSa[3]	209	8.25	1.73×10^8	7.06×10^4	8.63×10^4	2.66	377
LSb[4]	320	7.18	2.30×10^8	11.7×10^4	4.79×10^4	3.05	164
J[5]	288	12	3.5×10^8	46×10^4	6.7×10^4	1	900
H[6]	323				1.0×10^4	1	50
P[7]	500	4	2×10^8			1	1
NS[8]	352	6.75	2.37×10^8	28×10^4	28×10^4	1	1
WLC[9]	165	8.5	1.4×10^8	9×10^4	9×10^4	1.75	1.75
HS[10]	250	15	3.75×10^8	34×10^4	0.44×10^4	1	1
CHa[11]	258	6.31	1.62×10^8	18.1×10^4	18.1×10^4	1	1
CHb[12]	280	5.8	1.62×10^8	26.3×10^4	4×10^4	1	1
CHc[13]	256	6.33	1.62×10^8	16×10^4	4.3×10^4	1	1
CHd[14]	270	6.00	1.62×10^8	15.9×10^4	4.3×10^4	1	1
HB[15]	320	13	4.16×10^8	34×10^4	3.7×10^4	1	1

Footnote. Referring to Table 2.

[1] Chamberlain's [1960] solar breeze model, with the baropause conditions $r_o = 2.5\ R_S$, $T_e(r_o) = T_p(r_o) = 2 \times 10^6$ °K, $n_e(r_o) = 10^6\ cm^{-3}$.

[2] Sen's [1969] exospheric model with an electric sheath potential at the baropause $r_o = 6.05\ R_S$ and $T_e(r_o) = T_p(r_o) = 10^6$ °K, $n_e(r_o) = 3 \times 10^4\ cm^{-3}$.

[3] Kinetic model of Lemaire and Scherer with the same baropause conditions as in Sen's [1969] model.

[4] Kinetic model of Lemaire and Scherer fitting the most probable quiet solar wind flow speed and average proton temperature at 1 AU. The baropause conditions are $r_o = 6.6\ R_S$, $T_e(r_o) = 1.52 \times 10^6$ °K, $T_p(r_o) = 0.984 \times 10^6$ °K, $U_e = 0$, $U_p = 14\ km\ sec^{-1}$, $n_e(r_o) = 3.1 \times 10^4\ cm^{-3}$.

[5] Jockers' [1970] semikinetic model n° III, with baropause conditions $r_o = 2.5\ R_S$, $T_e(r \leq 9\ R_S) = 1.32 \times 10^6$ °K, $T_e(r > 9\ R_S) \propto r^{-1/3}$, $T_p(r_o) = 1.32 \times 10^6$ °K, $n_e(r_o) = 9 \times 10^5\ cm^{-3}$, $U_e = U_p = 0$.

[6] Semikinetic model calculated by Hollweg [1970] with baropause conditions $r_o = 15\ R_S$, $T_e(r) = 10^6$ °K, $T_p(r_o) = 10^5$ °K, $U_E = 0$, $U_p = 175\ km\ sec^{-1}$.

[7] Parker's [1958, 1963] isothermal one-fluid model, with a reference level $r_1 \approx 1\ R_S$, and $T_e(r) = T_p(r) = 10^6$ °K, $n_e(r_o) = 2 \times 10^8\ cm^{-3}$.

[8] Noble and Scarf's [1963] conductive one-fluid model, with isotropic gas pressure and $r_1 \approx 1\ R_S$, $T_e(r_1) = T_p(r_1) = 2 \times 10^6$ °K, $n_e(r_1) = 2 \times 10^8\ cm^{-3}$.

[9] Whang et al.'s [1966] conductive and viscous one-fluid model, with $r_1 \approx 1\ R_S$, $T_e(r_1) = T_p(r_1) = 1.5 \times 10^6$ °K, $n_e(r_1) = 2.8 \times 10^8\ cm^{-3}$.

[10] Hartle and Sturrock's [1968] conductive two-fluid model with isotropic gas pressure and $r_1 \approx 1\ R_S$, $T_e(r_1) = T_p(r_1) = 2 \times 10^6$ °K, $n_e(r_1) = 3 \times 10^7\ cm^{-3}$.

[11] Cuperman and Harten's [1970a] one-fluid model with reduced thermal conductivity beyond 15 R_S, $r_1 \approx 1\ R_S$, $n_e(r_1) = 2.65 \times 10^8\ cm^{-3}$, $T_e(r_1) = T_p(r_1) = 1.33 \times 10^6$ °K.

[12] Cuperman and Harten's [1970b] two-fluid model with enhanced noncollisional coupling between the protons and the electrons, $r_1 \approx 1\ R_S$, $T_e(r_1) = T_p(r_1) = 1.66 \times 10^6$ °K, $n_e(r_1) = 2.4 \times 10^7\ cm^{-3}$.

[13] Cuperman and Harten's [1971] two-fluid model with enhanced noncollisional coupling and reduced electron thermal conductivity, $r_1 \approx 1\ R_S$, $T_e(r_1) = 1.67 \times 10^6$ °K, $n_e(r_1) = 2.3 \times 10^7\ cm^{-3}$.

[14] Cupperman and Harten's [1971] two-fluid model with enhanced proton thermal conductivity and reduced electron thermal conductivity, $r_1 \approx 1\ R_S$, $T_e(r_1) = T_p(r_1) = 1.66 \times 10^6$ °K, $n_e(r_1) = 2.4 \times 10^7\ cm^{-3}$.

[15] Hartle and Barnes' [1971] conductive two-fluid model with isotropic gas pressure and an appropriated heating mechanism for the solar wind protons, $r_1 = 2\ R_S$, $T_e(r_1) = 1.5 \times 10^6$ °K, $T_p(r_1) = 1.2 \times 10^6$ °K, $n_e(r_1) = 1.5 \times 10^6\ cm^{-3}$.

CONCLUSIONS

If Pannekoek-Rosseland's polarization field is substituted by the correct electric field in the exospheric problem, quite reliable kinetic models can be obtained for the solar wind. The flow velocity, the density, the particle and energy fluxes, and the electron and proton temperatures of our kinetic models are in quite good agreement with the observed values for quiet solar wind conditions as given by Hundhausen [1968, 1969, 1970]. The deduced correlation of the proton and electron temperatures with the solar wind flow speed are supported by the observations reported by Burlaga and Ogilvie [1970] and Hundhausen et al. [1970]. Although the ratio of the parallel half-width temperature to the perpendicular half-width temperature is nearly equal to the observed temperature anisotropy, the corresponding ratio for the 'integrated' temperatures is however, much too large. As a consequence, plasma instabilities would probably destroy such large anisotropies in the velocity distribution. At 1 AU, Coulomb collisions can also contribute to reduce the large temperature anisotropies of a pure collisionless model. In the outermost part of the coronal exosphere ($r > 50 - 100\ R_s$), the ions and electrons probably will be scattered by wave-particle or particle-particle interactions and will no longer move freely in the gravitational and electrostatic fields, as it is assumed in our kinetic models. A similar conclusion has already been obtained by Eviatar and Schultz [1970] and by Griffel and Davies [1969].

Since the average electron and proton temperatures are correctly predicted in our model, we suggest that these interactions do not affect the bulk velocity or the mean kinetic energy of the electrons and protons but probably only change the pitch-angle distribution. Therefore, no external heating mechanism seems to be needed inside the exospheric region ($r > 6\text{-}7\ R_s$) to explain the quiet solar wind features. A heating mechanism is however, required up to 6 or 7 solar radii to keep the electron and

proton temperatures 1.5×10^6 °K and 0.98×10^6 °K, respectively, at 6 or 7 R_s [Hartle and Barnes, 1970] .

APPENDIX A : Boundary Conditions

In our kinetic model the electrons and protons are supposed to move freely in the external gravitational magnetic and electrostatic field. The electrons are distributed according to what Lemaire and Scherer [1970] have called a 'trapped model'. That distribution means that the electrons, which have two mirror points above the baropause r_o^+, are supposed to be in thermal equilibrium with the ballistic and escaping electrons. Since for $r > r_o^+$ the total potential energy for the protons is a monotonic decreasing function of the radial distance, no trapped or ballistic protons exist in our models.

If the velocity distribution at the baropause is given by (9) and if the incoming particles are excluded, it can be verified that N_e and N_p are not the actual electron and proton densities at r_o^+. This difference is due to the truncation of the velocity distribution function. For $U_e = 0$ one obtains

$$\lim_{r \to r_o^+} n_p(r) = bN_p = \frac{1}{2} \mathrm{Erfc}(- X)N_p \qquad \text{(A1)}$$

$$\lim_{r \to r_o^+} T_{\perp p}(r) = \theta_p \qquad \text{(A2)}$$

$$\lim_{r \to r_o^+} n_e(r) = cN_e$$

$$= \left(1 - \frac{1}{2} \mathrm{Erfc}\,(Y) - \frac{Y}{(\pi)^{1/2}} e^{-Y^2} \right) N_e \qquad \text{(A3)}$$

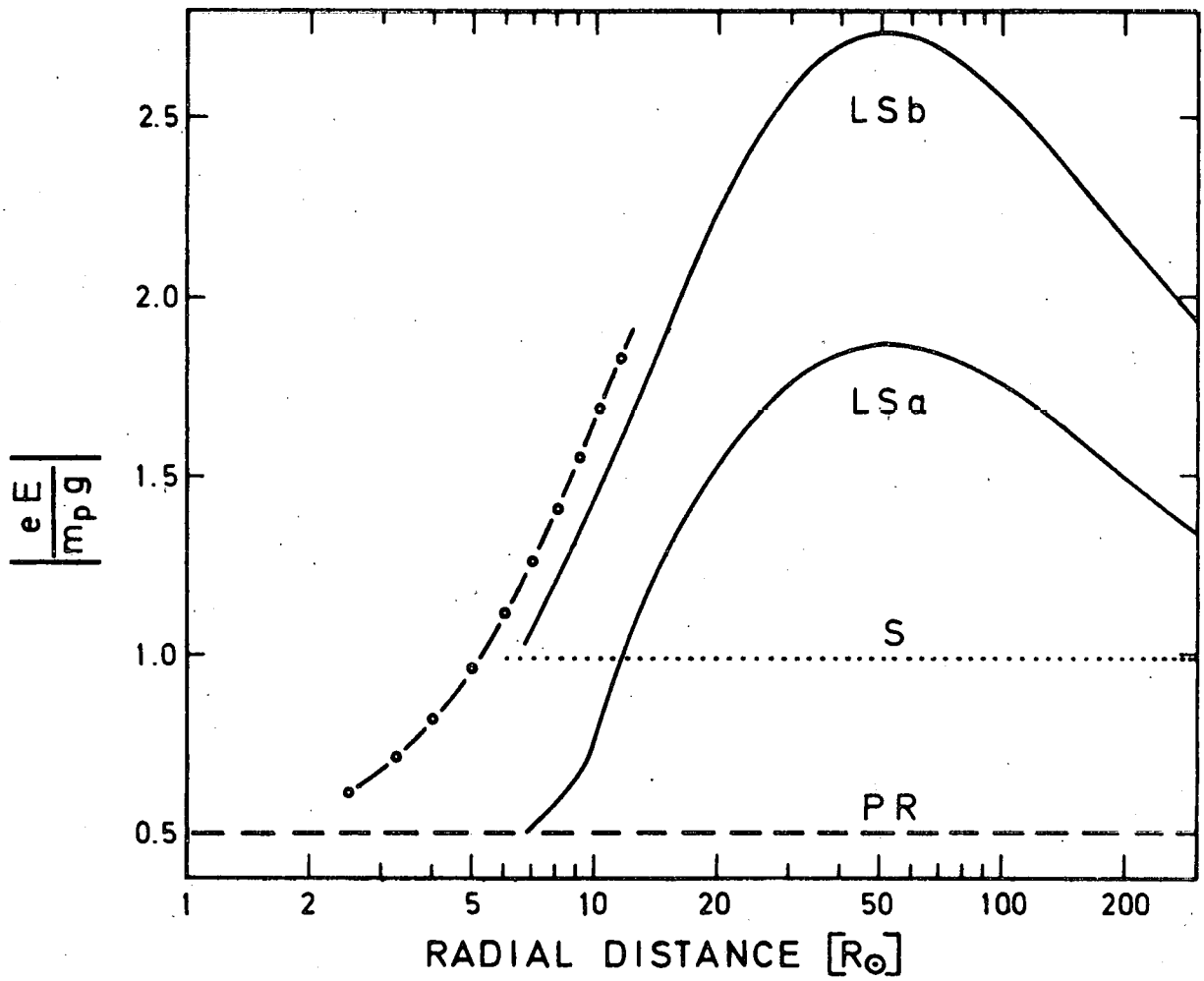

Fig. 7.- Ratio of the electric force to the gravitational force acting upon a proton, for different exospheric models of the solar corona. The dashed line (PR) corresponds to Pannekoek-Rosseland's potential ; the dotted line (S) represents the exospheric model calculated by Sen [1969] for $r_o = 6.05 R_\odot$ and $T_e(r_o) = T_p(r_o) = 10^6$ °K; the solid lines illustrate the results of Lemaire and Scherer : LSa corresponds to the same baropause conditions as in Sen's model, where LSb corresponds to $r_o = 6.6\ R_\odot$, $T_e(r_o) = 1.52 \times 10^6$ °K, $T_p(r_o) = 0.984 \times 10^6$ °K, $U_p = 14$ km sec^{-1}, and $U_e = 0$. The empirical values deduced from Pottasch's[1960] coronal density distribution are represented by open dots.

$$\lim_{r \to r_o^+} T_{\perp e}(r) = a\,\theta_e$$

$$= \frac{1 - \frac{1}{2}\,\mathrm{Erfc}\,(Y) - \frac{Y}{(\pi)^{1/2}} e^{-Y^2}\left(\frac{3}{2} + Y^2\right)}{1 - \frac{1}{2}\,\mathrm{Erfc}(Y) - \frac{Y}{(\pi)^{1/2}} e^{-Y^2}}\,\theta_e \tag{A4}$$

where we used the shorthand notations

$$X^2 = m_p U_p^{\,2}/2k\theta_p \tag{A5}$$

$$Y^2 = (GM\,m_e/k\theta_e r_o)(1 + \alpha_e) \tag{A6}$$

and where the complementary error function is defined by

$$\mathrm{Erfc}(y) = \frac{2}{(\pi)^{1/2}} \int_y^\infty e^{-x^2}\,dx \tag{A7}$$

G is the gravitational constant, and M is the mass of the sun. The constant α_e is related to the difference of electric potential between infinity and r_o,

$$\alpha_e = -\frac{e[\vec{\Phi}_E(\infty) - \vec{\Phi}_E(r_o)]}{GMm_e} \tag{A8}$$

The numerical value of α_e is obtained by solving (3), which for a proton-electron gas reduces to

$$\frac{1}{4} N_p \left(\frac{8k\theta_p}{\pi m_p}\right)^{1/2} [e^{-X^2} + (\pi)^{1/2} X\,\mathrm{Erfc}(-X)]$$

$$\frac{1}{4} N_e \left(\frac{8k\theta_e}{\pi m_e}\right)^{1/2} \left[1 + \frac{GMm_e}{k\theta_e r_o}(1 + \alpha_e)\right] \cdot \exp\left[-\frac{GMm_e}{k\theta_e r_o}(1 + \alpha_e)\right] \tag{A9}$$

APPENDIX B : Half-Width Temperatures

The velocity distribution of the protons in the exosphere is proportional to

$$\exp\left[- q - V_{\perp}^{2} - V_{//}^{2} - X^{2} + 2X \left[q + V^{2} + (1 + 1/\eta)\, V^{2}\right]^{1/2}\right. \tag{B1}$$

where

$$V_{\perp}^{2} = \frac{m_p v_{\perp}^{2}}{2k\theta_p} \qquad V_{//}^{2} = \frac{m_p v_{//}^{2}}{2k\theta_p} \tag{B2}$$

$$q = \frac{\left[m_p \Phi_g(r) + e\Phi_E(r)\right]_{r_o}^{r}}{k\theta_p} \tag{B3}$$

$$\eta = \frac{B(r)}{B(r_o)} \tag{B4}$$

B(r) is the magnetic field intensity at the radial distance r, and X is defined by (A5).

The most probable values of $|V_{\perp}|$, $V_{\perp}$, and $V_{//}$ are given by

$$|V_{\perp}|_M^{2} = \frac{1}{2} \tag{B5}$$

$$V_{\perp M} = 0 \tag{B6}$$

$$(V_{//M})^{2} = X^{2} - q + \frac{1 - \eta}{2} \tag{B7}$$

The half-width reduced velocities are obtained from

$$(V_{\perp,D})^{2} = 1.\eta\, 2 + \frac{2X^{2}}{\eta} - 2X\left(\frac{X^{2}}{2} - 1.\eta\, 2 \left(1 - \frac{1}{\eta} \right) \right)^{1/2} \tag{B8}$$

$$(V_{\perp D})^2 = \ln 2 + \frac{1-\eta}{2} - q + X^2 \pm 2X(\ln 2)^{1/2} \qquad \text{(B9)}$$

and the half-width temperatures are given by

$$\bar{T}_{\perp} = \theta_p [(V_{\perp D} - V_{\perp M})^2 / \ln 2] \qquad \text{(B10)}$$

$$\bar{T}_{\uparrow\uparrow} = \theta_p [(V_{\parallel D}' - V_{\parallel M})^2 / \ln 2] \qquad \text{(B11)}$$

$$\bar{T}_{\downarrow\downarrow} = \theta_p [(V_{\parallel M} - V_{\parallel D}'')^2 / \ln 2] \qquad \text{(B12)}$$

where $V_{\parallel D}'$ and $V_{\parallel D}''$ are the largest and smallest positive solutions of (B9), respectively.

These half-width temperatures are very sensitive to the value of the asymmetry parameter U_p. For instance, if $U_p = 0$, $\bar{T}_{\perp}(r) = \bar{T}_{\uparrow\uparrow}(r) = T_{\downarrow\downarrow}(r) = T_p(r_o)$. If however, the velocity distribution of the protons is highly asymmetric [$U_p^2 \tilde{>} (8k\theta_p/\pi m_p)$] at the baropause, the half-width temperature anisotropy $\bar{T}_{\uparrow\uparrow}/\bar{T}_{\perp}$ becomes as large as the pressure anisotropy, i.e., $T_{\parallel p}/T_{\perp p}$.

Acknowledgments. We would like to express our gratitude to Professor M. Nicolet for his valuable advice during the preparation of this work. One of the authors (J.L.) is very thankful to Professor P. Ledoux, who called his attention to the application of exospheric theories to the solar wind. We would also like to express our appreciation to the referees for their helpful suggestions.

* * * * *

REFERENCES

BERTOTTI, B., A. ROGISTER, and K. SCHINDLER, Absolute instability of whistler waves, Phys. Lett., in press, 1971.

BRANDT, J.C., Introduction to the Solar Wind, p.8, W.H. Freeman, San Fransisco, Calif. 1970.

BRANDT, J.C., and J.P. CASSINELLI, Interplanetary gas, 11, An exospheric model of the solar wind, Icarus, 5, 47, 1966.

BURLAGA, L.F., and K.W. OGILVIE, Heating of the solar wind, Astrophys. J., 159,659, 1970.

CHAMBERLAIN, J.W., Interplanetary gas, 2, Expansion of a model solar corona, Astrophys. J., 131, 47, 1960.

CUPERMAN, S., and A. HARTEN, The solution of one-fluid equations with modified thermal conductivity for the solar wind, Cosmic Electrodynamics, 1, 205, 1970a.

CUPERMAN, S., and A. HARTEN, Non-collisional coupling between the electron and proton components in the two-fluid model of the solar wind, Astrophys. J., 162, 315, 1970b.

CUPERMAN, S., A. HARTEN, The electron temperature in the two-component solar wind, Astrophys. J., 163, 383, 1971.

DESSLER, A.J., General applicability of solar-wind and solar breeze theories, Comments Astrophys. Space Phys., 1, 31, 1969.

EVIATAR, A., and M. SCHULZ, Ion-temperature anisotropies and the structure of the solar wind, Planet.Space Sci., 18, 321, 1970.

FORSLUND, D.W., Instabilities associated with heat conduction in the solar wind and their consequences, J. Geophys.Res., 75, 17, 1970.

GRIFFEL, D.H., and L. DAVIS, The anisotropy of the solar wind, Planet.Space Sci., 17, 1009, 1969.

HARTLE, R.E. and P.A. STURROCK, Two-fluid model of the solar wind, Astrophys. J., 151, 1155, 1968.

HARTLE, R.E., and A. BARNES, Non-thermal heating in the two-fluid solar wind, J. Geophys. Res., 75, 6915, 1970.

HOLLWEG, J.V., Collisionless solar wind, 1, Constant electron temperature, J. Geophys. Res., 75, 2403, 1970.

HOLLWEG, J.V., and H.J. VÖLK, Two new plasma instabilities in the solar wind, Nature, 225, 441, 1970.

HUNDHAUSEN, A.J., Direct observation of solar wind particles, Space Sci. Rev., 8, 99, 1968.

HUNDHAUSEN, A.J., Non-thermal heating in the quiet solar wind, J. Geophys. Res., 74, 5810, 1969.

HUNDHAUSEN, A.J., Composition and dynamics of the solar wind plasma, Rev. Geophys. Space Phys., 8, 729, 1970.

HUNDHAUSEN, A.J., S.J. BAME, J.R. ASBRIDGE, and S.J. SYDORIAK, Solar wind proton properties: Vela observations from July 1965 to June 1967, J. Geophys. Res., 75, 4643, 1970.

JENSEN, E., Mass losses through evaporation from completely ionized atmosphere with application to the solar corona, Astrophys. Norv., 8, 99, 1963.

JOCKERS, K., Solar wind models based on exospheric theory, Astron. Astrophys., 6, 219, 1970.

KENNEL, C.F., and F.L. SCARF, Thermal anisotropies and electromagnetic instabilities in the solar wind, J. Geophys. Res., 73, 6149, 1968.

LEMAIRE, J., and M. SCHERER, Le champ électrique de polarisation dans l'exosphère ionique polaire, C.R. Acad. Sci. Paris, Série B, 269, 666, 1969.

LEMAIRE, J., and M. SCHERER, Model of the polar ion exosphere, Planet. Space Sci., 18, 103, 1970.

LEMAIRE, J. and M. SCHERER, Phys. Fluids, 14, 1683, 1971.

MONTGOMERY, M.D., S.J., BAME, and HUNDHAUSEN, Solar wind electrons: Vela 4 measurements, J. Geophys. Res., 73, 4999, 1968.

NICOLET, M., G. KOCKARTS, and P.M., BANKS, Aeronomy, Handb. Physik, 49, p. 108, 1971.

NOBLE, L.M., and F.L. SCARF, Conductive heating of the solar wind, 1, Astrophys. J., 138, 1169, 1963.

PANNEKOEK, A., Ionization in stellar atmospheres, Bull. Astron. Inst. Neth., 1, 107, 1922.

PARKER, E.N., Dynamics of the interplanetary gas and magnetic fields, Astrophys. J., 128, 664, 1958.

PARKER, E.N., Interplanetary Dynamical Processes, p.73. Interscience, New York, 1963.

PELIPP, W., and H.J. VÖLK, Analysis of electromagnetic instabilities parallel to the magnetic field, J. Plasma Phys., 6, 1, 1971.

POTTASCH, S.R., Use of the equation of hydrostatic equilibrium in determining the temperature distribution in the outer solar atmosphere, Astrophys. J., 131, 68, 1960.

ROSSELAND, S., Electrical state of a star, Mon. Notic. Roy. Astron. Soc., 84, 720, 1924.

SEN, H.K.,The electric field in the solar coronal exosphere and the solar wind, J. Franklin Inst., 287, 451, 1969.

SPITZER, L., Jr., Physics of Fully Ionized Gases, p. 65, Interscience, New York, 1956.

VAN DE HULST, H.C., The Sun, edited by G.P. Kuiper, p. 306, University of Chicago Press, Chicago, Ill., 1953.

WHANG, Y.C.K. LIU, and C.C. CHANG, A viscous model of the solar wind, Astrophys. J., 145, 255, 1966.